Original Article

Outward potassium current in neurons of aestivated land snail *Achatina fulica*

Corrente externa de potássio em neurônios do caracol terrestre *Achatina fulica*

A. Mishchenko[a]*

[a] Shenzhen MSU-BIT University, Faculty of Biology, Shenzhen, China

Abstract

Aestivation and hibernation represent distinct forms of animal quiescence, characterized by physiological changes, including ion composition. Intracellular ion flows play a pivotal role in eliciting alterations in membrane potential and facilitating cellular communication, while outward K+ currents aid in the restitution and upkeep of the resting membrane potential. This study explores the relationship between inward and outward currents during aestivation in Achatina fulica snails. Specimens were collected near MSUBIT University in Shenzhen and divided into two groups. The first group was kept on a lattice diet, while the second one consisted of aestivating individuals, that were deprived of food and water until a cork-like structure sealed their shells. Recording of current from isolated neurons were conducted using the single-electrode voltage clamp mode with an AxoPatch 200B amplifier. Electrophysiological recordings on pedal ganglia neurons revealed significant differences in the inactivation processes of the Ia and Ikdr components. Alterations in the Ikdr component may inhibit pacemaker activity in pedal ganglion neurons, potentially contributing to locomotion cessation in aestivated animals. The KS current remains unaffected during aestivation. Changes in slow K+ current components could disrupt the resting membrane potential, possibly leading to cell depolarization and influx of Ca2+ and Na+ ions, impacting cell homeostasis. Thus, maintaining the constancy of outward K+ current is essential for cell stability.

Keywords: aestivation, inward current, Ikdr current, snail *Achatina*.

Resumo

A estivação e a hibernação representam formas distintas de quiescência animal, caracterizadas por alterações fisiológicas, incluindo a composição de íons. Os fluxos de íons intracelulares desempenham papel fundamental na provocação de alterações no potencial de membrana e na facilitação da comunicação celular, enquanto as correntes de K+ de saída ajudam na restituição e manutenção do potencial de membrana em repouso. Este estudo explora a relação entre as correntes de entrada e de saída durante a estivação em caracóis *Achatina fulica*. Os espécimes foram coletados perto da Universidade MSUBIT, em Shenzhen, e divididos em dois grupos. O primeiro grupo foi mantido em uma dieta de treliça, enquanto o segundo consistia em indivíduos estivados, que foram privados de alimento e água até que uma estrutura semelhante a uma rolha selasse suas conchas. O registro da corrente de neurônios isolados foi realizado usando o modo de grampo de tensão de eletrodo único com amplificador AxoPatch 200B. Os registros eletrofisiológicos nos neurônios dos gânglios pedais revelaram diferenças significativas nos processos de inativação dos componentes Ia e Ikdr. As alterações no componente Ikdr podem inibir a atividade do marcapasso nos neurônios do gânglio pedal, contribuindo potencialmente para a interrupção da locomoção em animais estivados. A corrente KS não é afetada durante a estivação. As alterações nos componentes da corrente lenta de K+ podem perturbar o potencial de membrana em repouso, possivelmente levando à despolarização celular e ao influxo de íons Ca2+ e Na+, afetando a homeostase celular. Portanto, manter a constância da corrente de K+ de saída é essencial para a estabilidade celular.

Palavras-chave: estivação, corrente interna, corrente Ikdr, caracol *Achatina*.

1. Introduction

Aestivativation and hibernation both represent forms of animal quiescence, characterized by a particular type of dormancy when the rates of metabolism, oxygen consumption and cellular energy demands are significantly suppressed (Navas and Carvalho, 2010). While hibernation is an adaptation to cold climates (Bui et al., 2023; Ugwuoke et al., 2022), aestivation is rather a strategy to cope with warm, dry conditions (Sheralieva et al., 2023; Zaitsev et al., 2024). In such circumstances, animals appear to enter a sleep-like state and cease feeding (Karmaliyev et al., 2023; Shevko et al., 2023). This is strategy of surveillance mechanism to endure

unfavorable environmental conditions (Kubenkulov et al., 2018; Kussainova et al., 2023; Mukhamadiyev et al., 2023; Nokusheva et al., 2023; Rahim et al., 2023).

Both aestivated and hibernated animals undergo general changes in their organism including alterations in cell metabolism, signaling, ion composition (Wang et al., 2015). In mammals, hibernation is associated with increasing activity of hippocampal neurons and inhibition of reticular formation neurons in the brain stem, leading to torpor bouts (Hamilton et al., 2017). The involvement of certain neuropeptides in regulating the hibernation state of mammals has been demonstrated. In response to decreased metabolic rate during aestivation of the African lungfish, there is an associated reduction in the activity of genes responsible for immune system function (Niu et al., 2023).

Dormancy is marked by alterations in ion channel activity. Studies on frog skin during hibernation demonstrated a decrease in Na^+ and Cl^- transport (Kosik-Bogacka and Tyrakowski, 2007). Investigations by Kiss et al. (2014) revealed a reduction in the inward Na^+ current in mollusk neurons during hibernation.

Inward ion currents, such as Na^+ and Ca^{2+}, play a crucial role in generating changes in membrane potential, including action potentials and gradual potentials (Jabeen et al., 2021). These currents are integral to transmission, providing information transfer between cells. This function is particularly vital for nervous cells that control the functional activity of other cells within an organism (Lehmann-Horn and Jurkat-Rott, 2003; Senatore et al., 2016). Conversely, outward current, provided by K^+ channels contribute to restoring the membrane potential to its resting level and maintaining the resting membrane potential (Battonyai et al., 2014). To explore the potential association between changes in inward current during aestivation and outward current, we investigated the outward current in the aestivated land snail *Achatina fulica*. We hypothesize, that the decreased activity of inward current during aestivation may be linked to changes in outward K^+ current.

2. Materials and Methods

Specimens of *Achatina fulica* were gathered from the vicinity of the MSUBIT University campus in Shenzhen in 2023 and categorized into two groups. The first group (16 animals) consisted of active snails housed in captivity and maintained on a lattice diet (Abdalla et al., 2023). The second group (12 animals) comprised aestivating individuals. Aestivation was induced by withholding water and food until a cork-like structure appeared, blocking the mollusk's shell. A total of 84 cells from active animals and 41 cells from aestivated animals were analyzed. The animals were studied two to three weeks after sealing their shells.

In electrophysiological researches the neurons of pedal ganglia were utilized. Deshelled animals were immersed for 10 minutes in the bath solution containing 2.5% Listerine. The subesophageal neural ring was isolated, and the paired pedal ganglia were separated from the rest of the ring. Collagenases I, II, and IV (2.5%) were applied to the

ganglia for 1 hour. After removing the outer connective tissue sheath, neurons were carefully isolated from each other through repeated pipetting. The neurons were sedimented at 2000 rotations per minute and washed twice with Hank's solution (200-220 mOsm) using the same sedimentation procedure (Santos and Boehs, 2021). These isolated neurons were subsequently placed in tissue culture dishes with cover glass for one hour, during which time the cells adhered to the glass surface.

Recording of current from isolated neurons were conducted using the single-electrode voltage clamp mode with an AxoPatch 200B amplifier. Electrodes with resistances ranging from 3.5 to 4.5 MΩ were prepared from fire-polished borosilicate glass capillaries (Satter Instrument) using a PC-100 (Narishige) drawing tube. These electrodes were filled with a pipette solution containing the following concentrations (in mM): 83 KCl, 10 $MgCl_2$, 5 EGTA, 10 HEPES, 2 MgATP, adjusted to a pH of 7.4. The bath solution contained the following (in mM): 85 NaCl, 9 KCl, 5 $CoCl_2$, 7 $MgCl_2$, 10 HEPES, 5 Glucose, 0.003 tetrodotoxin, also adjusted to a pH of 7.4. In some experiments the solutions containing $CaCl_2$ instead of $CoCl_2$ and without tetrodotoxin were used.

Series resistance and membrane capacity were online compensated. Only the cells with a membrane potential more negative than -40 mV were included in analysis. The membrane capacity of the cells averaged 51.6 ± 22.6 pF. Ion currents of each cell were normalized to the unit of membrane capacity and expressed as pA/pF. Data acquisition and analysis were performed using Axopatch, Clampfit 10.4, GraphPad Prism, and Excel software.

Ion channel conduction was calculated using the equation:

$$G = \frac{I}{Vm - Ek} \tag{1}$$

In this Equation 1, G is conduction, I is the current density, Vm is clamped potential, and Ek is the equilibrium potential for potassium (K+).

Ek was determined using the Nernst equation:

$$Ek = \left(\frac{RT}{zF}\right) * \ln\left(\frac{Kout}{Kin}\right) \tag{2}$$

In this Equation 2, R is the gas constant, T is the temperature in Kelvin, F is Faraday's constant, [K]out is the extracellular potassium concentration in the bath solution, and [K]in is intracellular potassium concentration in the pipette solution.

The data for K channel activation and inactivation were fitted by Boltzmann equation:

$$Vm = \frac{Imax}{1 + e^{(V50 - Vm)/Vc}} + C \tag{3}$$

In this Equation 3, f(V) represents the normalized to maximal value conduction, V50 is the membrane potential at which the ion current reaches half of its maximal value, Gmax is the maximal value of conduction, Vc is the slope factor, and C is a constant.

Statistical significances were assessed using student unpaired and paired t-tests, with differences considered significant at $p < 0.05$.

3. Results

The outward currents of all investigated neurons exhibited heterogeneity in the kinetics of activation and inactivation in response to depolarization voltage steps (DVSs). Examples of typical responses of a cell are depicted in Figure 1. The holding potential was maintained at -80 mV. Activation of outward currents was induced by DVSs ranging from -100 mV to 100 mV in 10 mV increments. All components of the outward current showed an increase with enhanced depolarization.

Three main components of the outward current were identified: a very fast component Ia (I_{to}), and slower components I_{kdr} and KS. To activate the very fast I_a current, a hyperpolarization step to -110 mV was applied prior to the DVSs. To inactivate the Ia component, either a predepolarization 600 ms step to -50 mV or a predepolarization 200 ms step to -20 mV were applied prior to the DVS.

When a pre-depolarization to -50 mV (for 600 ms) was applied instead of hyperpolarization, the very fast component Ia became undetectable. The remaining currents are identified as I_{kdr} and KS components. The I_{kdr} component demonstrated fast inactivation but with a slower rate compared to the Ia component. The KS current demonstrated very slow inactivation and was analyzed at the end of recording protocol. Subtracting data recorded with hyperpolarizing and depolarizing steps prior to DVSs allowed isolating only the I_a component without I_{kdr} and I_s. It is characterized by prominent fast inactivation during a short time.

The application of tetraethylammonium chloride (TEACl, 30 mM) led to suppression of the I_{kdr} and KS components of the outward currents. The maximal inhibitory effect of TEACl was observed at DVS ranging from -30 to +100 mV, with the degree of inhibition reaching 57.8% ± 3.5% for Ikdr current and 63.3 ± 4.7% for KS current. The I_a current was not significantly inhibited by TEACl. Similar to experiments without TEACl, pre-depolarization to -50 mV or -20 mV in presence of TEACl resulted in the prominent suppression of the I_a current (Figure 1).

The I-V relationships of all three components of the outward currents are presented in Figure 2. The very fast Ia component is activated at voltage clamped above -50 mV, whereas higher (above -20 mV) depolarization is required to activate both I_{kdr} and KS components. To compare the responses of active and aestivated snails, we conducted a statistical analysis of current densities for I_a, I_{kdr} and KS in a general set of neurons. We also examined neuron populations with relatively high and low current densities, as well as groups of cells with higher and lower
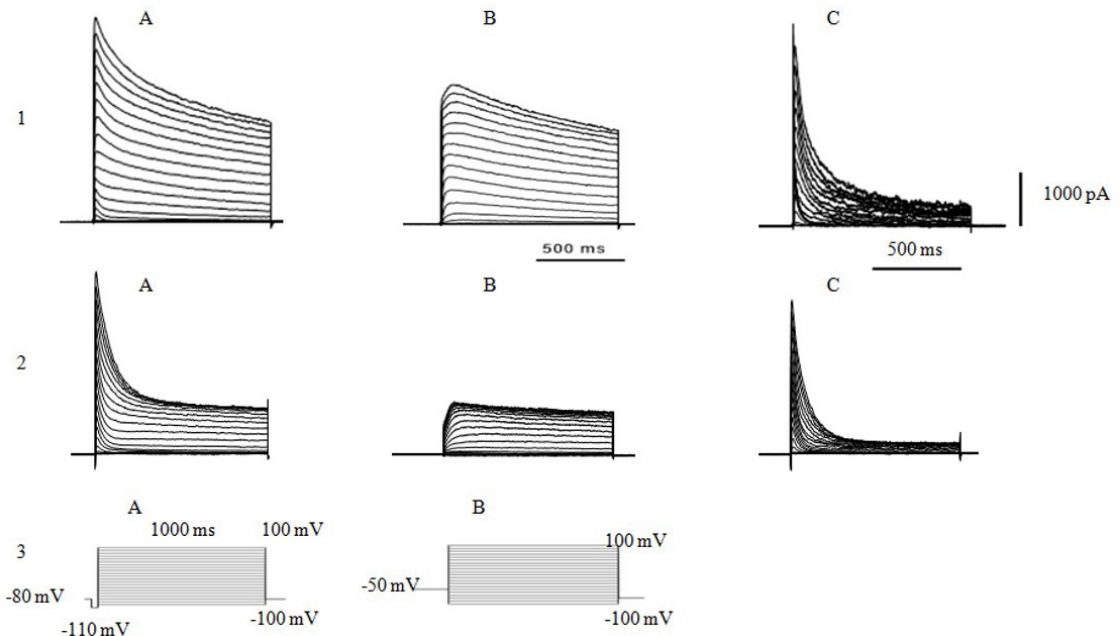
Figure 1. Outward currents recorded in the pedal ganglion neuron in response to the DVS application. 1 - Currents are recorded in a normal physiological solution. (A) Very fast outward currents (Ia) were activated by a prior hyperpolarization to -110 mV; (B) In the same cell, a 600 ms pre-depolarization to -50 mV causes inactivation of Ia component. Remaining currents represent Ikdr and slow Is components; (C) The isolated Ia component of the outward current was obtained by subtracting B from A. 2 - Application of TEACl (30 mM). (A) Ia component of the outward current was initiated with a 200 ms hyperpolarization to -110 mV; (B) Outward currents were recorded with a 600 ms pre-depolarization to -50 mV. Compared with recording without TEACl (1B), Ikdr component is suppressed; (C) Isolated Ia component in presence of TEACl was obtained by subtracting A from B. 3 - Pulse protocols used to activate outward currents. (A) Pulse protocol for the activation of the Ia current; (B) Pulse protocol used to inactivate the Ika current for recording Ikdr and Is currents.
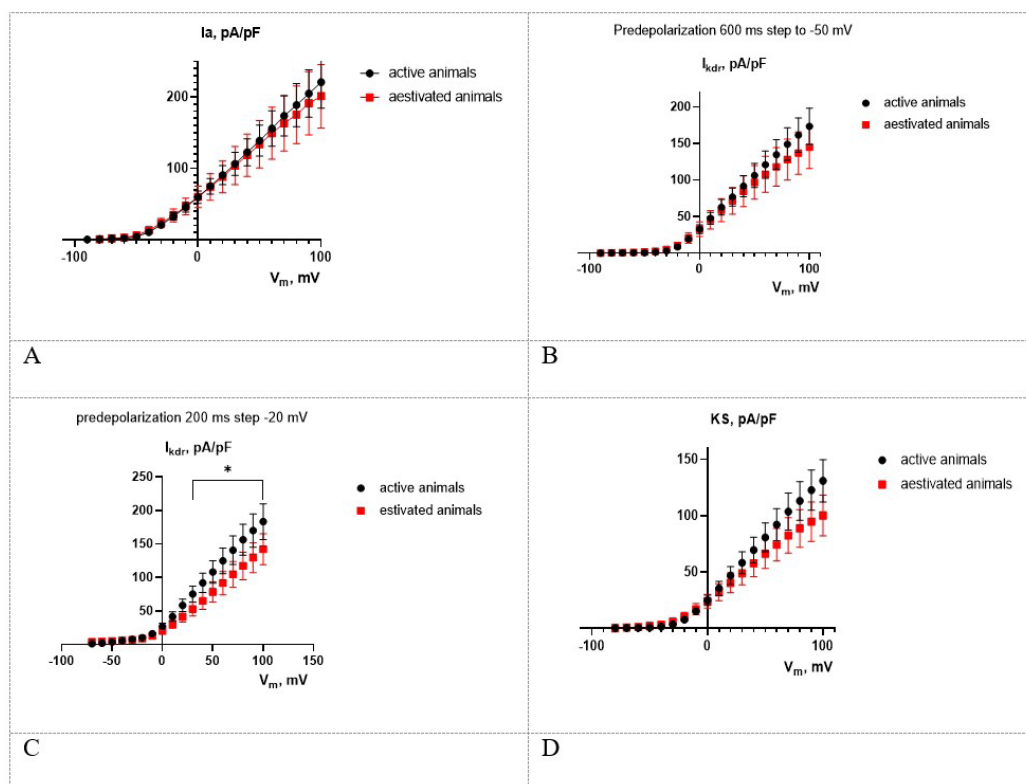
Figure 2. I-V characteristics of the fast and slow outward current components in the neurons from both active and aestivated animals (mean ± SD). (A) Ia component of ion currents was recorded when hyperpolarization to -110 mV was followed by DVSs; (B) Ikdr component of ion currents was recorded when 600 ms depolarization to -50 mV was followed by DVSs; (C) Ikdr component of ion currents was recorded when 200 ms depolarization to -20 mV was followed by DVSs; (D) KS component was analyzed at the end of first recording currents.

membrane capacity. None of these approaches revealed any differences in Ia and Is responses between active and aestivated animals (Figure 2).

The same results were obtained for Ikdr when initiated by DVSs followed by pre-depolarization to -50 mV. Only Ikdr recorded in experiments when pre-depolarization to -20 mV was applied showed lower current density in aestivated animals compared to active animals at potentials higher than 40 mV. In fact, the current density of aestivated animals was lower by 26.9±9.5 pA/pF, 33.3±12.7 pA/pF, 39.1±15.3 pA/pF at fixed potentials +40 mV, +60 mV and +80 mV respectively.

To compare K$^+$ channel activation in neurons of active and aestivated snails, the conductions of fast and slow components of the outward current were calculated. The obtained values were used to plot normalized conduction as a function of membrane potential. These data were then fitted with the Boltzmann equation to determine the slope factor (V_c) and voltage causing 50% current activation (V_{50}) (Figure 3).

Similar to I-V relationships, the V_{50} value for I_{kdr} and I_s components were shifted to more positive potentials compared to those for I_a current. The data indicated no differences in the V_{50} and V_c of I_a and I_{kdr} in the neurons of active and aestivated animals. The average value of V_{50} for

the I_a component was -18 ± 7.1 mV and -27.6 ± 11 mV in active and aestivated animals, respectively. V_{50} for I_{kdr} component when a pre-depolarization step to -50 mV was applied, constituted 6.3 ± 4.3 mV in active animals and 0.5 ± 2.9 mV in aestivated animals. V50 of I_{kdr} component stimulated by the application of a pre-depolarizing step to -20 mV resulted in V_{50} shifting to 17.8 ± 3.2 mV in active animals and 23.4 ± 5.9 mV in aestivated animals. The slope factor varied from approximately 30 (I_a component) to approximately 20 (I_{kdr} component) and also demonstrated similarities between active and aestivated animals. These data suggest that there are no changes in the activation kinetics of K$^+$ channels when active animals enter aestivation.

To exam the steady-state inactivation of the fast component, we conducted experiments using the inactivation protocol. Initially, cells were depolarized to 30 mV (control response). This step was followed by DVSs applied to potentials ranging from -90 to +20, lasting for 5 seconds to inactivate the fast currents. These were followed by a test stimulus to 30 mV caused the activation of the rest of non-inactivated K$^+$ channels. The results were plotted as Itest/Icontrol, demonstrating the steady-state inactivation (Figure 4).
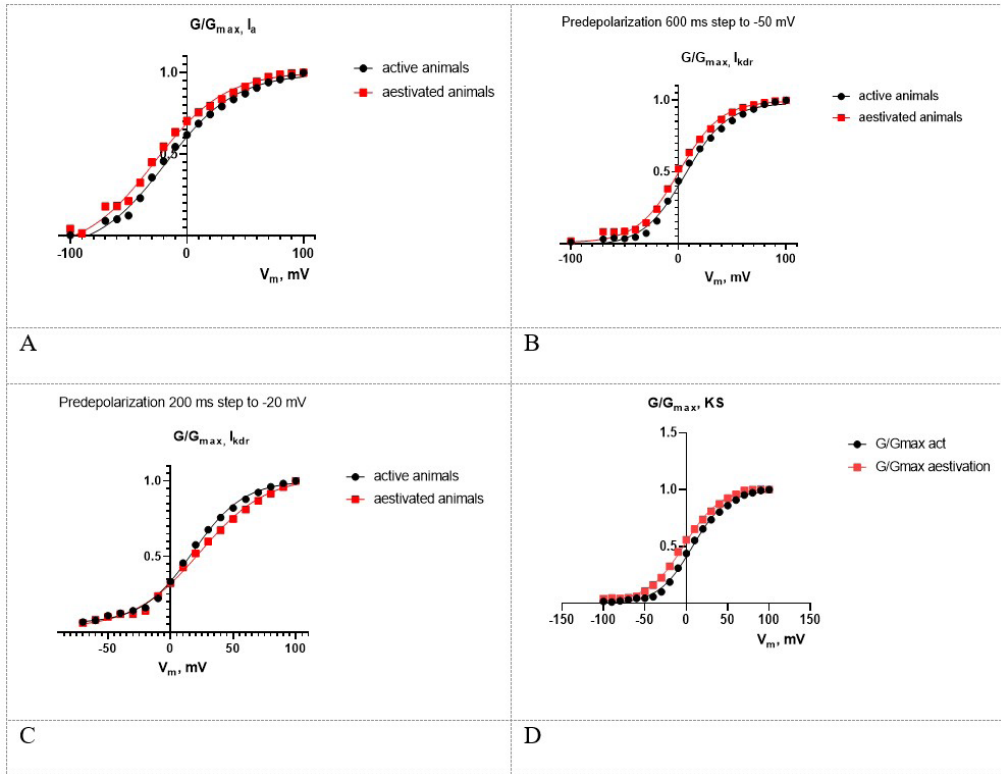
Figure 3. Activation of K+ channels was analyzed as normalized conductivity G/Gmax in respect to clamped potentials. (A) G/Gmax for the very fast component activated by a preceding hyperpolarizing step to -110 mV; (B) G/Gmax for the Ikdr component. A pre-depolarization of 600 ms to -50 mV precedes the application of DVSs; (C) G/Gmax for the Ikdr component. Pre-depolarization of 200 ms to -20 mV was followed by DVSs; (D) G/Gmax for the KS component.
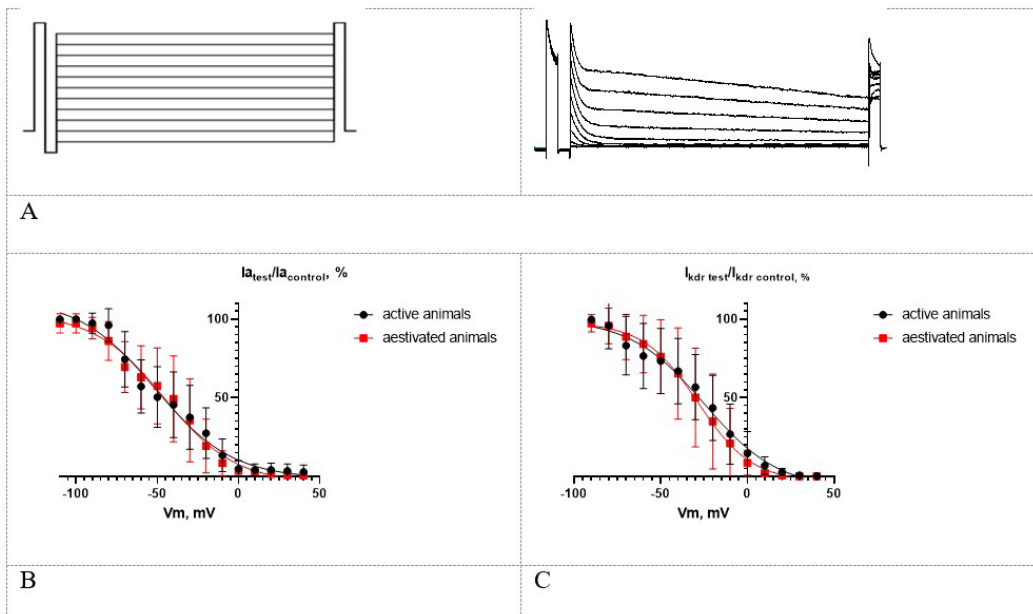
Figure 4. Steady-state inactivation of the fast Ia and Ikdr outward current components. (A) The left part: pulse protocol employed for studying the process of inactivation. First depolarization step to 30 mV (control stimulus) is followed by DVSs and second depolarization step to 30 mV (test stimulus). The right part: recorded ion currents; (B) Steady-state inactivation of the Ia component in active animals compared to aestivated animals (Mean ± SD); (C) Steady-state inactivation of the Ikdr component in active animals compared to aestivated animals (Mean ± SD).
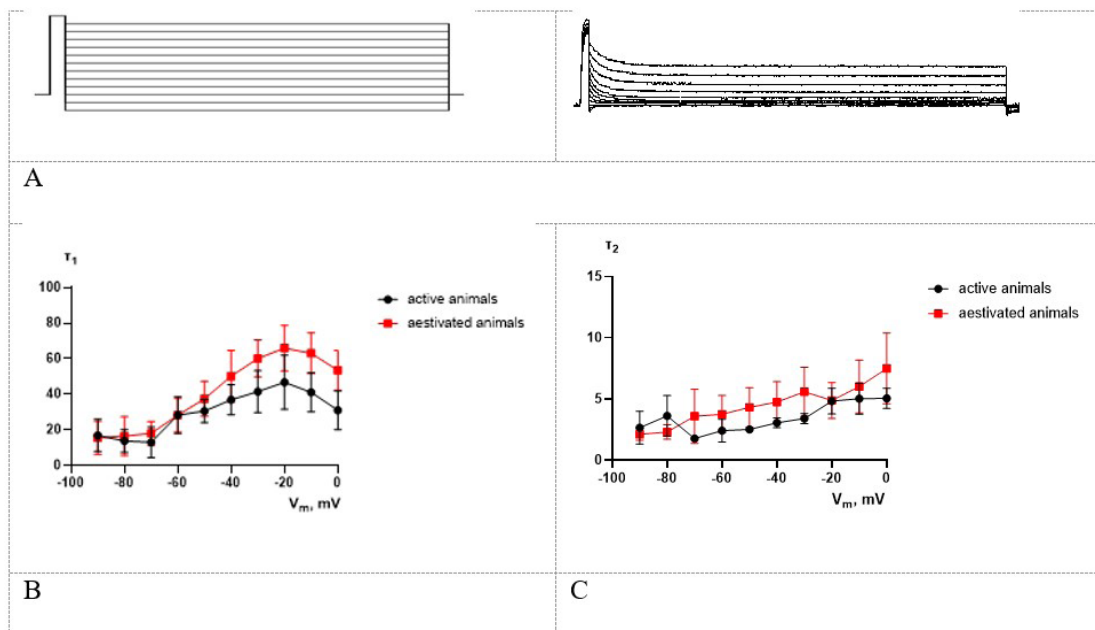
Figure 5. Kinetics of deactivation of outward current in neurons from both active and aestivated animals. (A) The left part: deactivation protocol: A 200 ms depolarization to 50 mV precedes the voltage steps ranging from -90 to 10 mV. The right part: recorded ion currents; (B) τ_1 plotted against voltage steps (Mean ± SD); (C) τ_2 plotted against voltage steps (Mean ± SD).

The data revealed significant differences between the processes of inactivation for the Ia component and the Ikdr component. For active snails, half of the inactivation for Ia was observed at potentials between -51.3 ± 8.8, while half of the inactivation for Ikdr occurred at potentials -24.8 ± 9.9; the slope factor did not differ significantly between the Ia and Ikdr components (23.8 ± 8.2 and 21.4 ± 11.2 respectively), Furthermore, we did not find any differences in the processes of inactivation between active animals and aestivated animals by analyzing V_{50} (in aestivated snails V_{50} values constituted -45.5 ± 9.8 for I_a component and -28.6 ± 7.9 for I_{kdr} component). Also we didn't find any differences in V_c of I_a current (23.8 ± 8.2 in active animals vs. 21.9 ± 9.5 in aestivated animals). The I_{kdr} component demonstrated a decrease in V_c due to aestivation by 26.7% (respective V_c values for I_{kdr} current were 21.4 ± 11.2 in active snails vs. 15.7 ± 8.1 in aestivated snails).

The process of deactivation was assessed with application the deactivation pulse protocol to the cells. This protocol involved a 200 ms depolarization to 50 mV, followed by returning the potential to values ranging from -90 to 0 mV in 10 mV steps (Figure 5). The deactivation process was well-fitted by an exponential equation with two time constants, $\tau 1$ and $\tau 2$, indicating its complexity, possibly due to the involvement of different types of potassium channels. No differences were discovered between aestivated and active animals when analyzing both $\tau 1$ and $\tau 2$. For example, $\tau 1$ values were 46.8 ± 15.2 and 65.9 ± 12.8 in active and aestivated snails, respectively, when the subsequent depolarization step was -20 mV. The corresponding values of $\tau 2$ were 4.8 ± 2.3 and 4.9 ± 4.2 in active and aestivated snails.

4. Discussion

The different aspects of the outward current in the pedal ganglia neurons of the land snail *Achatina fulica* were comprehensively analyzed. Mollusk neurons have long served as a classic model for investigation these ion currents (Kuroda and Abe, 2020; Zolfaghari and Vatanparast, 2020). The presence of several types of outward currents (Battonyai et al., 2014; Hofmeier and Lux, 1979) as well as inward Na^+ currents (Gilly et al., 1990, 1997; Hernandez et al., 2017) and inward Ca^{2+} currents (Kits and Mansvelder, 1996; Pirger et al., 2010; Tosti et al., 2022) has been demonstrated in neurons of different snail species.

Our data reveal the complexity of outward current in the neurons. Identifying three main types of outward currents: a transitional very fast activating/inactivating component Ia (or Ito), Ikdr and KS. Similar components have been demonstrated in neurons of both invertebrates and vertebrates (Gilly et al., 1997; Koyama and Appel, 2006a, b; Windley et al., 2011). In our experiments, Ikdr and KS components exhibited high sensitivity to TEACl (30mM) consistent with the findings of Thompson (1977) in *Tritonia* neurons and Hermann and Gorman (1981) in *Aplysia* neurons. Ia component was suppressed with predepolarization rather than with TEACl.

Prior studies have revealed that hibernation induces notable changes in the electrophysiological responses of various cells. In hibernating mammals, a significant decrease the Ca^{2+} current in cardiomyocytes has been detected (Wang et al., 2002). This decrease is attributed to the reduction in cAMP-dependent phosphorylation of Ca^{2+} channels. Additionally, neurons of hibernated mollusks have shown the suppression of Na^+ current associated
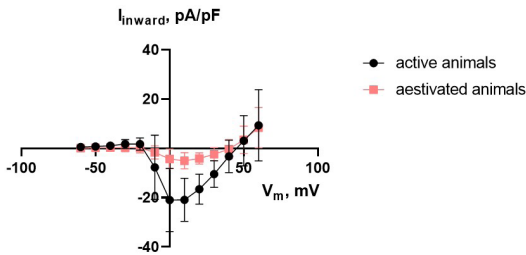
Figure 6. I-V characteristic of inward current components in neurons of both active and aestivated animals (Mean ± SD). To register the inward currents, the cells were supplemented with bath solution containing 5 mM Ca^{2+} and without tetrodotoxin.

with a decrease in Na^+ channels in the cell membranes (Kiss et al., 2014). While we didn't conduct a detailed analysis of Na^+ and Ca^{2+} currents in aestivated *Achatina* neurons, measurements of inward current density in several cells (n=9 for active animals and n=8 for aestivated animals) were carried out without discrimination of Na^+ and Ca^{2+} components (Figure 6). Despite the insufficient number of cells for detailed statistical analysis, our records demonstrated a prominent decrease in inward current in aestivated animals compared with active animals, aligning with the findings of Kiss et al. (2014). Biological significance of inward current suppression is that both, Na^+- and Ca^{2+}- currents provide the action potential generation in pacemaker cells (Kononenko and Kostyuchenko, 2001; Lu and Feng, 2011). Such pacemaker activity decreasing may be associated with general decreasing locomotion of snails during aestivation.

The fast components of outward K^+ are involved in action potential generation, especially in cells with spontaneous activity (Dougalis et al., 2017; Wu et al., 2008). Both Ia and Ikdr can be considered as components that are crucial for pacemaker cell functions, but we observed suppression only in Ikdr component when applied predepolarization step to -20 mV prior to DVSs. This suppression was evident from complex changes of K^+ channel functions: decreasing the amplitude of the ion current density, changes of the parameters determined in processes of inactivation. For example, decrease in current density could suggest that fewer channels are contributing to the outward K+ current. This may be considered to be resulted from less expression of K^+ channels in neurons during aestivation. The decrease in slope factor during inactivation may indicate that the remaining in the cell membrane channels become more sensitive to changes in voltage. The last is proposed due to changes in the ion channel composition or the ration of different types of ion channels.

5. Conclusion

In general given the association of the Ikdr component with spontaneous activity, we propose that changes in Ikdr components may be linked to the inhibition of pacemaker activity in pedal ganglion neurons, potentially contributing to the cessation of locomotion in aestivated animals.

The KS current was not affected during aestivation. Because the main function of the slow components of K^+ current is to maintain the resting membrane potential, changes in slow components could initiate it's alterations. Against the background of energy shortages in the cells of aestivated animals (and therefore, active transport through the cell membrane), possible depolarization due to membrane potential alterations can lead to the entrance of Ca^{2+} and Na^+ ions into the cells (Wood and Baker, 2001), resulting in cell swelling and affecting Ca^{2+} signaling. Hence, it's important or the cell to prevent the changes in membrane potential because the constancy of the slow component of outward K^+ current is crucial for maintaining cell homeostasis.

In general, our data indicate the changes some components of Ikdr current initiated by snail *Achatina* transition to aestivation state.

References

ABDALLA, S.F., ELNOUR, L.Y., ABDULAZIZ, N.M., IDRIES, A.H., OSMAN, M.E.M. and KONOZY, E.H., 2023. Lawsonia inermis seeds cotyledon and coat extracts as a potential antimicrobial agent. *Advancements in Life Sciences*, vol. 10, no. 2, pp. 270-275.

BATTONYAI, I., KRAJCS, N., SERFÖZÖ, Z., KISS, T. and ELEKES, K., 2014. Potassium channels in the central nervous system of the snail, Helix pomatia: localization and functional characterization. *Neuroscience*, vol. 268, pp. 87-101. http://doi.org/10.1016/j.neuroscience.2014.03.006. PMid:24631713.

BUI, A.P.N., TAM, T.L.H., PHUONG, P.T. and LINH, N.T., 2023. Overdominance in livestock breeding: examples and current status. *Advancements in Life Sciences*, vol. 10, no. 4, pp. 525-529.

DOUGALIS, A.G., MATTHEWS, G.A.C., LISS, B. and UNGLESS, M.A., 2017. Ionic currents influencing spontaneous firing and pacemaker frequency in dopamine neurons of the ventrolateral periaqueductal gray and dorsal raphe nucleus (vlPAG/DRN): a voltage-clamp and computational modeling study. *Journal of Computational Neuroscience*, vol. 42, no. 3, pp. 275-305. http://doi.org/10.1007/s10827-017-0641-0. PMid:28367595.

GILLY, W.F., GILLETTE, R. and MCFARLANE, M., 1997. Fast and slow activation kinetics of voltage-gated sodium channels in molluscan neurons. *Journal of Neurophysiology*, vol. 77, no. 5, pp. 2373-2384. http://doi.org/10.1152/jn.1997.77.5.2373. PMid:9163364.

GILLY, W.F., LUCERO, M.T. and HORRIGAN, F.T., 1990. Control of the spatial distribution of sodium channels in giant fiber lobe neurons of the squid. *Neuron*, vol. 5, no. 5, pp. 663-674. http://doi.org/10.1016/0896-6273(90)90220-A. PMid:2171590.

HAMILTON, J.S., CHAU, S.M., MALINS, K.J., IBANEZ, G.G., HOROWITZ, J.M. and HORWITZ, B.A., 2017. Syrian hamster neuroplasticity mechanisms fail as temperature declines to 15 °C, but histaminergic neuromodulation persists. *Journal of Comparative Physiology. B, Biochemical, Systemic, and Environmental Physiology*, vol. 187, no. 5-6, pp. 779-791. http://doi.org/10.1007/s00360-017-1078-5. PMid:28391591.

HERMANN, A. and GORMAN, L.F., 1981. Effect of tetraethylammonium on potassium currents in a molluscan neuron. *The Journal of General Physiology*, vol. 78, no. 1, pp. 87-110. http://doi.org/10.1085/jgp.78.1.87. PMid:6265594.

HERNANDEZ, J.S., WAINWRIGHT, M.L. and MOZZACHIODI, R., 2017. Long-term sensitization training in Aplysia decreases the excitability of a decision-making neuron through a sodium-

dependent mechanism. *Learning & Memory*, vol. 24, no. 6, pp. 257-261. http://doi.org/10.1101/lm.044883.116. PMid:28507035.

HOFMEIER, G. and LUX, H.D., 1979. Inversely related behaviour of potassium and calcium permeability during activation of calcium-dependent outward currents in voltage-clamped snail neurones. *The Journal of Physiology*, vol. 287, pp. 28-29. PMid:430408.

JABEEN, F., YOUNIS, T., SIDRA, S., MUNEER, B., NASREEN, Z., SALEH, F., MUMTAZ, S., SAEED, R.F. and ABBAS, A.S., 2021. Extraction of chitin from edible crab shells of Callinectes sapidus and comparison with market purchased chitin. *Brazilian Journal of Biology = Revista Brasileira de Biologia*, vol. 83, e246520. http://doi.org/10.1590/1519-6984.246520. PMid:34468518.

KARMALIYEV, R., NURZHANOVA, F., SIDIKHOV, B., MURZABAEV, K., SARIYEV, N., SATYBAYEV, B. and ABIROVA, I., 2023. Epizootiology of opisthorchiasis in carnivores, fish and mollusks in the West Kazakhstan Region. *American Journal of Animal and Veterinary Sciences*, vol. 18, no. 2, pp. 147-155. http://doi.org/10.3844/ajavsp.2023.147.155.

KISS, T., BATTONYAI, I. and PIRGER, Z., 2014. Down regulation of sodium channels in the central nervous system of hibernating snails. *Physiology & Behavior*, vol. 131, pp. 93-98. http://doi.org/10.1016/j.physbeh.2014.04.026. PMid:24769022.

KITS, K.S. and MANSVELDER, H.D., 1996. Voltage gated calcium channels in molluscs: classification, Ca^{2+} dependent inactivation, modulation and functional roles. *Invertebrate Neuroscience*, vol. 2, no. 1, pp. 9-34. http://doi.org/10.1007/BF02336657. PMid:9372153.

KONONENKO, N.I. and KOSTYUCHENKO, O.V., 2001. Mechanisms of generation of pacemaker activity by identified Helix neurons. *Neurophysiology*, vol. 33, no. 1, pp. 40-54. http://doi.org/10.1023/A:1010464230977.

KOSIK-BOGACKA, D.I. and TYRAKOWSKI, T., 2007. Effect of hibernation on sodium and chloride transport in isolated frog skin. *Folia Biologica*, vol. 55, no. 1, pp. 47-51. http://doi.org/10.3409/173491607780006317. PMid:17687934.

KOYAMA, S. and APPEL, S.B., 2006a. A-type K current of dopamine and GABA neurons in the ventral tegmental area. *Journal of Neurophysiology*, vol. 96, no. 2, pp. 544-554. http://doi.org/10.1152/jn.01318.2005. PMid:16611837.

KOYAMA, S. and APPEL, S.B., 2006b. Characterization of M-current in ventral tegmental area dopamine neurons. *Journal of Neurophysiology*, vol. 96, no. 2, pp. 535-543. http://doi.org/10.1152/jn.00574.2005. PMid:16394077.

KUBENKULOV, K., KHOKHANBAEVA, N. and NAUSHABAYEV, A., 2018. Comparative ameliorative efficiency of phosphogypsum and elemental sulfur in semi-terrestrial soda and sulfate moderately halophytic solonetz of the light gray earth subzone. *Online Journal of Biological Sciences*, vol. 18, no. 2, pp. 169-175. http://doi.org/10.3844/ojbsci.2018.169.175.

KURODA, R. and ABE, M., 2020. The pond snail Lymnaea stagnalis. *EvoDevo*, vol. 11, no. 1, pp. 24. http://doi.org/10.1186/s13227-020-00169-4. PMid:33292457.

KUSSAINOVA, M., TOISHIMANOV, M., SYZDYK, A., TAMENOV, T., NURGALI, N. and CHEN, J., 2023. Influence of time conditions on the soil temperature indicators in Kazakhstan. *Caspian Journal of Environmental Sciences*, vol. 21, no. 5, pp. 1117-1122.

LEHMANN-HORN, F. and JURKAT-ROTT, K., 2003. Nanotechnology for neuronal ion channels. *Journal of Neurology, Neurosurgery, and Psychiatry*, vol. 74, no. 11, pp. 1466-1475. http://doi.org/10.1136/jnnp.74.11.1466. PMid:14617700.

LU, T.Z. and FENG, Z., 2011. A sodium leak current regulates pacemaker activity of adult central pattern generator neurons in Lymnaea stagnalis. *PLoS One*, vol. 6, no. 4, e18745. http://doi.org/10.1371/journal.pone.0018745. PMid:21526173.

MUKHAMADIYEV, N.S., CHADINOVA, A.M., SULTANOVA, N., MENGDIBAYEVA, G.Z. and ANUARBEKOV, K.K., 2023. Development of environmentally friendly protection measures against pests and diseases. *Online Journal of Biological Sciences*, vol. 23, no. 2, pp. 243-250. http://doi.org/10.3844/ojbsci.2023.243.250.

NAVAS, C.A. and CARVALHO, J.E., eds., 2010. *Aestivation: molecular and physiological aspects*. Berlin: Springer.. http://doi.org/10.1007/978-3-642-02421-4.

NIU, Y., GUAN, L., WANG, C., JIANG, H., LI, G. and YANG, L., 2023. Aestivation induces widespread transcriptional changes in the African lungfish. *Frontiers in Genetics*, vol. 14, pp. 1096929. http://doi.org/10.3389/fgene.2023.1096929. PMid:36733343.

NOKUSHEVA, Z.A., KANTARBAYEVA, E.Y., ORMANBETOV, M.B., YERMAGAMBET, B.T., KASSENOVA, Z.M. and KAZANKAPOVA, M.K., 2023. Development and implementation of effective schemes for the use of mineral fertilizers in the forest-steppe zone of the North Kazakhstan Region. *Online Journal of Biological Sciences*, vol. 23, no. 3, pp. 313-322. http://doi.org/10.3844/ojbsci.2023.313.322.

PIRGER, Z., KISS, T., BATTONYAI, I. and ELEKES, K., 2010. Sodium-channel and membrane current characteristics of the procerebral neurons of Helix pomatia. In: *Proceedings of the Frontiers in Neuroscience: IBRO International Workshop*, 21-23 January 2010, Pécs, Hungary. Switzerland: Frontiers. http://doi.org/10.3389/conf.fnins.2010.10.00117.

RAHIM, S., HASNI, K., BALOCH, A.H., NAWAZ, A., WAJID, C., TARIQ, S., HASNI, M.S. and JAN, M., 2023. Variation analysis of Acanthopagrus Latus found in the coastal belt of Lasbella by using mitochondrial DNA, D-Loop region. *Advancements in Life Sciences*, vol. 10, no. 1, pp. 42-47.

SANTOS, G.B.M. and BOEHS, G., 2021. Chemical elements in sediments and in bivalve mollusks from estuarine regions in the south of Bahia State, northeast Brazil. *Brazilian Journal of Biology = Revista Brasileira de Biologia*, vol. 83, e249641. http://doi.org/10.1590/1519-6984.249641. PMid:34550292.

SENATORE, A., RAISS, H. and LE, P., 2016. Physiology and evolution of voltage-gated calcium channels in early diverging animal phyla: cnidaria, placozoa, porifera and stenophora. *Frontiers in Physiology*, vol. 7, pp. 481. http://doi.org/10.3389/fphys.2016.00481. PMid:27867359.

SHERALIEVA, Z., NURALIYEVA, U., KARYMSAKOV, T., TADZHIYEV, K., MOLDAKHMETOVA, G. and TADZHIYEVA, A., 2023. Climate zones and morphometric parameters of Apis mellifera carnica bees. *American Journal of Animal and Veterinary Sciences*, vol. 18, no. 4, pp. 243-248. http://doi.org/10.3844/ajavsp.2023.243.248.

SHEVKO, V.M., UTEEVA, R.A., BADIKOVA, A.B., KARATAEVA, G.E. and BITANOVA, G.A., 2023. Production of ferroalloys, calcium carbide, and phosphorus from high-silicon phosphorite. *Rasayan Journal of Chemistry*, vol. 16, no. 2, pp. 955-963. http://doi.org/10.31788/RJC.2023.1628310.

THOMPSON, S.H., 1977. Three pharmacologically distinct potassium channels in molluscan neurons. *The Journal of Physiology*, vol. 265, no. 2, pp. 465-488. http://doi.org/10.1113/jphysiol.1977.sp011725. PMid:850203.

TOSTI, E., BONI, R. and GALLO, A., 2022. Pathophysiological responses to conotoxin modulation of voltage-gated ion currents. *Marine Drugs*, vol. 20, no. 5, pp. 282. http://doi.org/10.3390/md20050282. PMid:35621933.

UGWUOKE, J.I., NWANKWO, C.A. and DIM, C.E., 2022. Phytomicrobial dietary treatment improves growth indices of pigs. *International Journal of Veterinary Science*, vol. 11, no. 2, pp. 257-263. http://doi.org/10.47278/journal.ijvs/2021.105.

WANG, S.Q., LAKATTA, E.G., CHENG, H. and ZHOU, Z.Q., 2002. Adaptive mechanisms of intracellular calcium homeostasis in

mammalian hibernators. *The Journal of Experimental Biology*, vol. 205, no. 19, pp. 2957-2962. http://doi.org/10.1242/jeb.205.19.2957. PMid:12200399.

WANG, T., SUN, L. and CHEN, M., 2015. Aestivation and regeneration. *Developments in Aquaculture and Fisheries Science*, vol. 39, pp. 177-209. http://doi.org/10.1016/B978-0-12-799953-1.00011-8.

WINDLEY, M.J., ESCOUBAS, P., VALENZUELA, S.M. and NICHOLSON, G.M., 2011. A novel family of insect-selective peptide neurotoxins targeting insect large-conductance calcium-activated K channels isolated from venom of the theraphosid spider *Eucratoscelus constrictus. Molecular Pharmacology*, vol. 80, no. 1, pp. 1-13. http://doi.org/10.1124/mol.110.070540. PMid:21447641.

WOOD, J.N. and BAKER, M., 2001. Voltage-gated sodium channels. *Current Opinion in Pharmacology*, vol. 1, no. 1, pp. 17-21. http://doi.org/10.1016/S1471-4892(01)00007-8. PMid:11712529.

WU, S.N., CHEN, B.S., LIN, M.W. and LIU, Y.C., 2008. Contribution of slowly inactivating potassium current to delayed firing of action potentials in NG108-15 neuronal cells: experimental and theoretical studies. *Journal of Theoretical Biology*, vol. 252, no. 4, pp. 711-721. http://doi.org/10.1016/j.jtbi.2008.01.031. PMid:18387636.

ZAITSEV, V., KOROTKIY, V., BOGOLYUBOVA, N., ZAITSEVA, L. and RYZHOV, V., 2024. Prevention of heat stress in lactating cows. *American Journal of Animal and Veterinary Sciences*, vol. 19, no. 1, pp. 7-12. http://doi.org/10.3844/ajavsp.2024.7.12.

ZOLFAGHARI, Z. and VATANPARAST, J., 2020. Thymol provokes burst of action potentials in neurons of snail Caucasotachea atrolabiata. *Comparative Biochemistry and Physiology. Toxicology & Pharmacology: CBP*, vol. 228, pp. 108654. http://doi.org/10.1016/j.cbpc.2019.108654. PMid:31683013.